Asian Journal of Chemistry; Vol. 28, No. 5 (2016), 1031-1034

ASIAN JOURNAL OF CHEMISTRY

http://dx.doi.org/10.14233/ajchem.2016.19577

Extraction and Characterization of Wrinkled Graphene Nanolayers from Commercial Graphite

A.V. RAMYA, B. MANOJ* and ANU N. MOHAN

Department of Physics, Christ University, Bangalore-560 029, India

*Corresponding author: E-mail: manoj.b@christuniversity.in

Received: 24 August 2015; *Accepted*: 12 October 2015; *Published online*: 30 January 2016; AJC-17741

A report on the synthesis of wrinkled graphene nano carbon from bulk graphite is presented here. The obtained graphene nano carbon comprises mixed phase, sp^2-sp^3 bonded disordered carbon network. The as synthesized samples were intercalated by Hummer's method and are separated by centrifugation and sonication to obtain few layer graphene sheets. The structural and chemical changes of the nanostructure was elucidated by Raman spectroscopy, XRD, SEM-EDS, XPS, FTIR and UV-Vis-NIR spectroscopy. Raman spectra confirmed the existence of highly graphitized amorphous carbon with five peaks in the deconvoluted first order Raman spectrum. The IR and XPS analysis confirms the incorporation of functional groups to graphitic basal plane. There was a shift in the peaks position and intensity with intercalation. The synthesized graphene sheet is found to be in the graphite to nanocrystalline graphitic trajectory. The SEM analysis revealed the formation of large area wrinkled graphene sheets. The nanostructure formed is effortlessly scalable and ideally suitable for nano carbon composites based nano electronic devices and switches.

Keywords: Graphene, Nanosheets, Mixed phase, Carbon.

INTRODUCTION

Graphene, a monolayer carbon atom with honey comb lattice structure, is reported to possesses exceptional properties [1,2]. Being the mother of all graphitic systems, it is the exciting topic of investigation in the present decade. Graphene is monolayer carbon, but bilayer or multi layers carbon is also explored with similar curiosity. Laboratory synthesis of nanostructural carbon has been carried out by many research groups in recent times [1-6]. To highlight few significant methods include chemical vapour deposition, mechanical exfoliation and reduction of graphene oxide. Bulk amount of graphene sheets can be easily produced by reducing graphene oxide (GO) [7,8]. Commonly used precursor for graphene is commercial graphite, a natural mineral, has to be purified to eliminate heteroatomic impurity. It comprises numerous, localized defects, that assist as seed point for oxidation process. The complexity and inherent defect of flake graphite, make the elucidation of precise oxidation mechanism very exciting. The oxidation can be controlled by altering the reaction method, synthesis conditions or the precursor. During this process, oxygen functional groups break the sp^2 hybridization of carbon network leading to the formation of sp^3 hybridization, which makes them predominantly amorphous. Oxidation of graphite generates defects in the stacked graphene sheets, which manifest as wrinkles in the stack thereby increasing the distance between adjacent sheets. Reduction of graphene layers remove sp^3 sites and restore sp^2 hybridization, referred to as graphitization.

Studies on disordered structures in graphene are important for the development of fundamental and applied science [2]. This disorder can be extrinsic, inherent defects and/or coexistence of sp^2-sp^3 carbon network which can induce alteration in the various properties of graphene owing to the alteration in the π-interactions of the honey comb lattice [2,9,10]. The coexistence of crystalline and amorphous carbon exhibited fascinating properties of the mixed structure [5]. The nanocarbon composites shows significant enhancement in physical properties and electrical conductivity. Unfortunately scalability of such mix mode structure is difficult. Commercial application evolve rapidly once sufficient quality of mixed structure is easily available. They find wide future applications in nano electrical applications and super capacitors.

In the present study, few layer graphene nano carbon (GNC) network is attained from flake graphite sheet by Hummer's method. The as synthesized samples were inoculated and sonicated. These samples were analyzed with the aid of Raman spectroscopy, Scanning electron microscopy and X-ray diffraction. The composition was also investigated using Fourier transform infrared spectroscopy, X-ray photoelectron spectroscopy, Ultraviolet-visible-near infrared spectroscopy (UV-Vis-NIR) and electron dispersion spectroscopy.

EXPERIMENTAL

Preparation of graphene sheets: Graphene nano carbon sheets were synthesized using flake graphite as precursor. 2 g of the graphite powder was mixed with 2 g of sodium nitrate and 100 mL of sulphuric acid and stirred continuously for 15 min in an ice bath. About 12 g of $KMnO_4$ was added to the mixture slowly and further cooled for 0.5 h. Further the solution was stirred continuously for 48 h in a Teflon coated magnetic stirrer. This was further mixed with 184 mL of distilled water, 560 mL of warm water along with 40 mL of H_2O_2 and the mixture was left out for 12 h. The graphene oxide particles formed were separated from the solution by centrifugation and washed repeatedly with water and acetone followed by sonication for a period of 20 min.

Chemical and structural elucidation: The sample was dispersed in isopropyl alcohol solution and sonicated to make them a uniform suspension. A few drops of solution were spread on Si-substrate using a micropipette. After drying, the sample was subjected to following analysis. The Raman measurements were carried out at 514.5 nm using Horiba LABAM-HR spectrometer. The surface morphology of sample was analyzed with JSM-6360 A (JEOL) system operated at 20 kV. The compositional analysis of the samples were performed with the aid of FT-IR-Alpha-T, Bruker spectrometer over the range 1000-3500 cm^{-1}, X-ray photo electron spectroscopy (XPS-Omicron ESCA probe) and UV-Vis-NIR spectrometer (Shimadzu).

RESULTS AND DISCUSSION

The XRD profile of as obtained graphite flakes (GS) is presented in Fig. 1. The prominent peak at 26.77° is an indication of crystalline carbon, while the spike at 44.76° is attributed to the hexagonal graphitic carbon [4]. The crystallite size (L_a) and the stacking height (L_c) of graphite flakes are calculated by modified Scherrer formula and is found to be 16.74 and 15.14 nm, respectively. The number of aromatic lamellae (N) in graphite flakes is calculated to be 6 while the carbon atoms per aromatic lamellae (n) is estimated as 11 [12-14].

The graphite powder after Hummers treatment was ultrasonicated for 30 min at room temperature followed by 20 min at 50 °C (sonicated graphite sheets). To probe the effect of sonication on structure, X-ray analysis was performed (Fig. 2). The peak at 26.33°, attributed to the (002) plane of ordered hexagonal graphite structure, has become narrower upon sonication, indicating the presence of crystalline graphitic carbon. The crystallite size (L_a) and the stacking height (L_c) of sonicated graphite sheets are lowered to 12.09 nm and 14.48 nm respectively. Sonication has resulted in the exfoliation of graphite into thin graphene layers. The d_{002}-spacing of the lamellae has increased to 3.38 Å. The number of aromatic lamellae (N) is calculated to be 6 while "n" is evaluated to be 11.

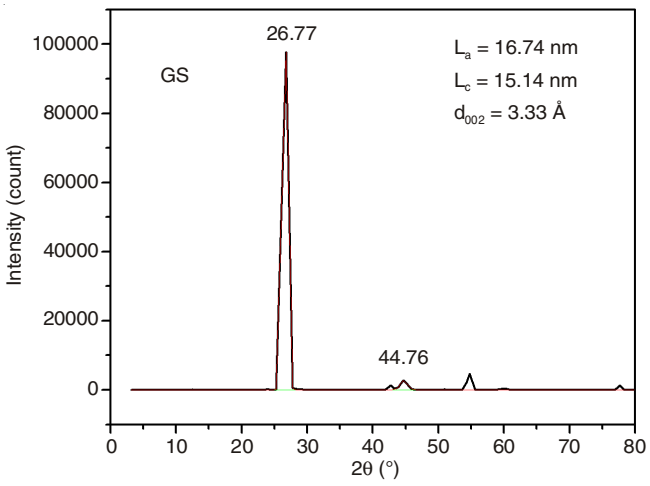

Fig. 1. XRD spectrum of graphite flakes

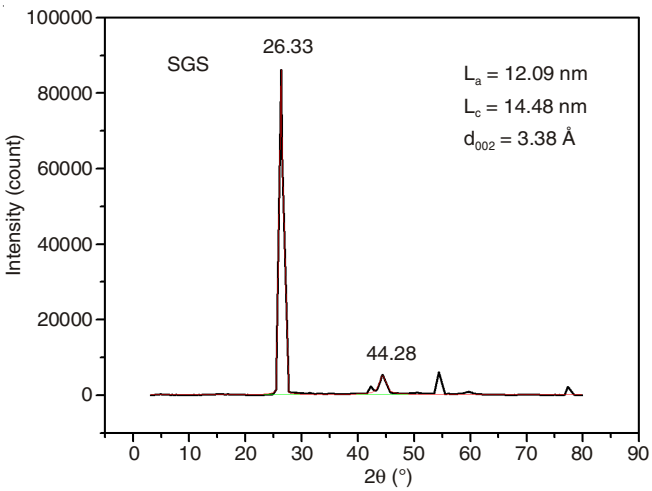

Fig. 2. XRD pattern of sonicated graphite sheets (SGS)

Raman spectrum of as received graphite flake is displayed in Fig. 3. It exhibited defect (D) and graphitic (G) bands at 1354 and 1584 cm^{-1} and an overtone 2D band at about 2716 cm^{-1} [2]. The ratio I_D/I_G of graphite flakes is calculated to be 0.29, indicating less defect for the graphene layers.

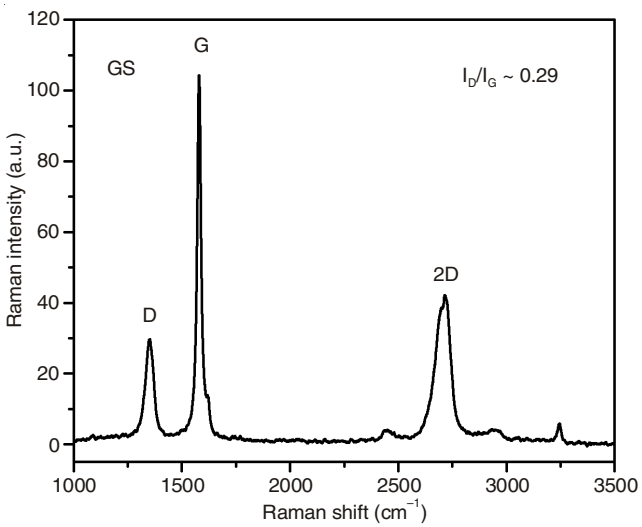

Fig. 3. Raman spectrum of graphite flakes (GS)

The flake graphite is intercalated by modified Hummer's method and is analyzed with Raman spectroscopy (Fig. 4). It reveals two overlying D and G bands at 1356 cm^{-1} and 1610 cm^{-1} and a broad 2D hump at about 2700 cm^{-1}. Increase in magnitude of D-band is likely due to the incorporation of functional

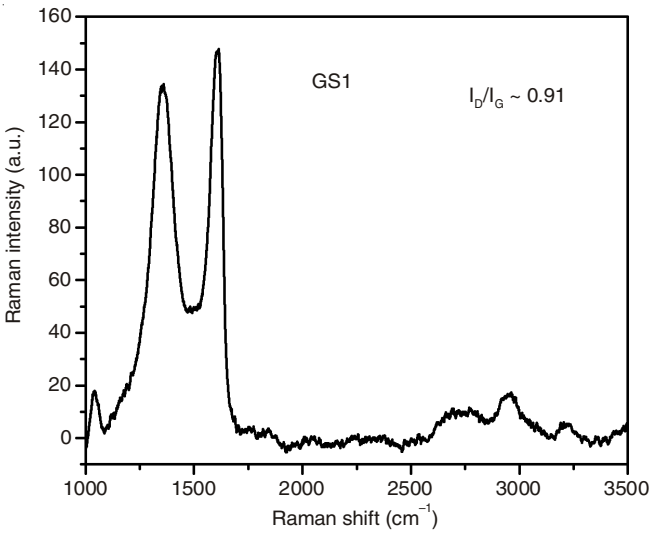

Fig. 4. Raman spectrum of intercalated graphite (GS1)

groups in the carbon backbone [12,13]. I_D/I_G ratio of intercalated graphite is increased to 0.91 due to the defects caused by various functional groups [10-16].

First order Raman spectrum (intercalated graphite) is deconvoluted to establish presence different structures of carbon atoms (Fig. 5). A total of five peaks were fitted and designated as G, D1, D2, D3 and D4. G band at about 1590 cm^{-1} also comprises the D2 band (at about 1618 cm^{-1}, known to arise from graphitic lattices). D1 band at about 1380 cm^{-1} has been due to lattice disturbance or edge of a graphene layer [2]. D3 band at about 1520 cm^{-1} originates from the amorphous carbon fraction (a-C). D4 band at about 1340 cm^{-1} is likely due to the mixed vibrations of sp^2-sp^3 bonds or C–C and C=C stretching [15-22]. These two band could also arises to finite size of crystallites or increase in defects by oxidation. Hence it can be concluded that finite size, less defective, few layer graphene oxide is formed as a result of oxidative treatment of graphite flakes.

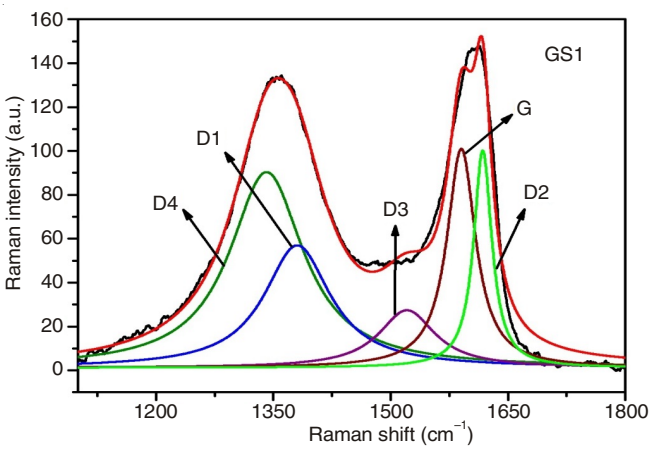

Fig. 5. Deconvoluted first order Raman spectrum of intercalated graphite

Following changes are observed after Hummer's method. (i) D band appears and I_D/I_G increases; (b) D2 band appears; (c) all peaks were broadened. The D and 2D peaks lose their doublet structure and become more broadened. The G and D bands are so wide that they start to overlap confirming the formation of nanocrystalline graphitic domain in the sample [3]. The peak observed at 1025 cm^{-1} in the sample is ascribed to the diamond phase (sp^3-phase) [1]. This is an indication that nanocrystalline graphite with less sp^3 content is developed with chemical intercalation.

UV-visible spectrum of graphite flakes is shown in Fig. 6. The absorbance peak observed at about 224 nm arises due to the π-π* plasmon peak of C-C and C=C bonds in sp^2 hybrid regions. This band confirms the stacking of graphene layers. This plasmon peak attributed to the following conjugative effect: primarily to the nanometer sized grapene cluster or to the linking of carbon and oxygenated functional groups. The shoulder band at 245 nm is due to n–π* transition of the C=O bond in sp^3 hybrid regions [22,23].

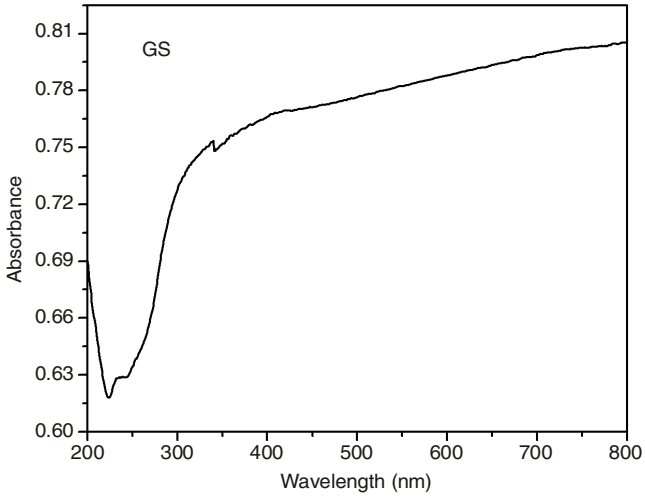

Fig. 6. UV-visible spectrum of graphite flakes (GS)

The wide band observed between 3500 and 3100 cm^{-1} is attributed to the hydroxyl stretching vibrations of the C-OH groups and the absorbed water molecules (Fig. 7). The peak observed at 1629 cm^{-1} is owing to the combined effect of C=C skeletal vibrations from graphitic domains, C=O stretching vibrations of COOH groups in the ketone or quinone groups [12,13].

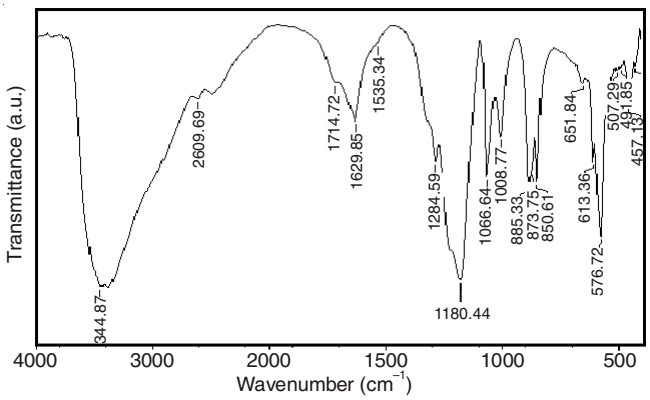

Fig. 7. FTIR spectrum of intercalated graphite (GS1)

The peak at 1535 cm^{-1} is due to C-C stretching vibration and O-H deformation. Another peak centered at 1180 cm^{-1} is associated with C-O stretching vibration of epoxide group, owing to incorporation of oxide functional groups after the intercalation. The adsorption bands at 885 to 850 cm^{-1} are

credited to C-H oop bending vibration. Spikes at 650 and 613 cm^{-1} arises from C-H bending vibration [17-21].

The deconvoluted XPS spectrum indicates carbon atoms in different functional groups: the non-oxygenated ring C, *i.e.,* the sp^2 carbon (about 284.7 eV), the C in C-O bonds, C bound to O either as epoxy or hydroxyl (about 286.0 eV), the carbonyl C, *i.e.,* C=O of alcohols, phenols or ether (about 287.5 eV) and the carboxylate carbon, O-C=O (about 288.9 eV) [22,23]. The π-π* satellite peak (about 290.1 eV) is also observed [23]. O1s in inset appears at 532.6 eV and mainly contributed from C=O (531.2 eV), C(=O)-(OH) (531.2 eV) and C-O (533 eV) [22,23]. From the XPS spectrum, the incorporation of functional groups in sp^2 nanocarbon can be deduced, which is also supported by FTIR and UV results.

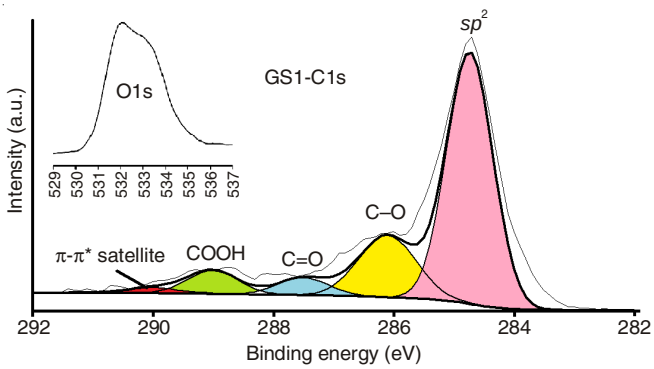

Fig. 8. XPS spectrum of nanographite (intercalated graphite)

Conclusion

In the current study, graphite and graphite oxide were examined by various characterization techniques. X-ray diffraction and Raman analyses reveal that graphite possesses crystalline graphitic structure with very little disorder. Scanning electron microscopy portrays graphite flakes as stacked layers of graphene. Sonication of graphite flakes resulted in further improved stacking of the graphene layers, which is in agreement with the XRD analysis. Hummer's treatment successfully incorporated oxygen functional groups in, which is supported by FTIR, XPS and EDS analyses. The chemical groups eventually increased the amount of disorder in intercalated graphite, as is evident from the Raman analysis. The number of graphene layers was computed to be 6 from XRD studies. Sonication of intercalated graphite has resulted in the reduction of graphite oxide and delamination of graphene sheets. SEM images of sonicated intercalated graphite disclose a cluster of wrinkled graphene islands. Graphene nano sheets has been prepared by the oxidation–reduction of graphite oxide and sonication of graphene oxide. The graphite (G) and defect band (D) are so wide that they start to overlap after the chemical intercalation. This is an indication of the formation of graphite to nanocrystalline graphitic domain in the sample. The mixed structure formed is scalable, economically viable and is best suited in the application of carbon based composites for electrochemical applications.

REFERENCES

1. S. Kumar, S. Patil, A. Joshi, V. Bhoraskar, S. Datar and P. Alegaonkar, *Appl. Surf. Sci.*, **271**, 86 (2013).
2. A. Sadezky, H. Muckenhuber, H. Grothe, R. Niessner and U. Pöschl, *Carbon*, **43**, 1731 (2005).
3. A. Kaniyoor, T.T. Baby, T. Arockiadoss, N. Rajalakshmi and S. Ramaprabhu, *J. Phys. Chem. C*, **155**, 17660 (2011).
4. A.N. Mohan and B. Manoj, *Int. J. Electrochem. Sci.*, **7**, 9537 (2012).
5. M. Balachandran, *Am. J. Anal. Chem.*, **5**, 367 (2014).
6. M. Terrones, A.R. Botello-Méndez, J. Campos-Delgado, F. López-Urías, Y.I. Vega-Cantú, F.J. Rodríguez-Macías, A.L. Elías, E. Muñoz-Sandoval, A.G. Cano-Márquez, J.-C. Charlier and H. Terrones, *Nanotoday*, **5**, 351 (2010).
7. K.S. Subrahmanyam, S.R.C. Vivekchand, A. Govindaraj and C.N.R. Rao, *J. Mater. Chem.*, **18**, 1517 (2008).
8. B. Manoj and A.G. Kunjomana, *J. Miner. Mater. Charact. Eng.*, **9**, 919 (2010).
9. B. Manoj, *J. Environ. Res. Develop.*, **9**, 209 (2014).
10. Y. Dong, J. Lin, Y. Chen, F. Fu, Y. Chi and G. Chen, *Nanoscale*, **6**, 7410 (2014).
11. C.D. Elcey and B. Manoj, *J. Univ. Chemical Technol. Metall.,* **45**, 385 (2010).
12. B. Manoj, *J. Min. Mater. Metallurgy*, **21**, 940 (2014).
13. B. Manoj, *Asian J. Chem.*, **26**, 4553 (2014).
14. B. Manoj and A.G. Kunjomana, *IOP Conf. Ser.: Mater. Sci. Eng.*, **73**, 012096 (2015).
15. A.K. Geim, *Science*, **324**, 1530 (2009).
16. A.V. Ramya, J. John and B. Manoj, *Int. J. Electrochem. Sci.*, **8**, 9421 (2013).
17. B. Manoj and A.G. Kunjomana, *Asian J. Mater. Sci.*, **2**, 204 (2010).
18. B. Manoj and A.G. Kunjomana, *Trends Appl. Sci. Res.*, **7**, 434 (2012).
19. N. Ponni and B. Manoj, *J. Miner. Mater. Charact. Eng.*, **1**, 39 (2013).
20. C.D. Elcey and B. Manoj, *Res. J. Chem. Environ.*, **17**, 11 (2013).
21. B. Manoj and A.G. Kunjomana, *Russ. J. Appl. Chem.*, **87**, 1726 (2014).
22. M. Huang, H.N. Lim, C.H. Chia, M.A. Yarmo and M.R. Muhamad, *Int. J. Nanomed.*, **6**, 3443 (2011).
23. Y. Wang, L. Xie, J. Sha, Y. Ma, J. Han, S. Dong, H. Liu, C. Fang, S. Gong and Z. Wu, *J. Mater. Sci.*, **46**, 3611 (2011).